PARAMETER
JURNAL MATEMATIKA, STATISTIKA DAN TERAPANNYA

e-ISSN. 2829-6303
Vol. 04 No. 2, August 2025
Pages 223-238

Fractional Modeling of the Interaction Between Mycobacterium Tuberculosis and Its Response to Antibiotics

Inayah Alifah Khairiah[1], Yudi Ari Adi[2]*

[1,2]Department of Mathematics, Faculty of Applied Science and Technology, Universitas Ahmad Dahlan, JAhmad Yani Street, Banguntapan, Bantul, Yogyakarta, 55191, Indonesia

E-mail Correspondence Author: *yudi.adi@math.uad.ac.id*

Abstract

Mycobacterium tuberculosis is a bacterium that causes tuberculosis, which is the second most common infectious disease in the world and generally attacks the lungs. It is important to formulate the dynamics of interactions and the effects of antibiotic administration on Mycobacterium tuberculosis into a mathematical model, especially using a fractional order approach. In this study, a model was developed using the Caputo-Fabrizio derivative. The purpose of the study was to study the dynamics of interactions between bacteria and antibiotics, where the administration of antibiotics causes the bacterial population to be divided into two types, namely sensitive bacteria and bacteria resistant to antibiotics. Based on the model built, four equilibrium points were obtained. Stability analysis shows that these equilibrium points are locally asymptotically stable under certain conditions. To support the results of the analysis, numerical simulations were carried out using the three-step Adams-Bashforth method with the Caputo-Fabrizio derivative. The simulation results showed that the smaller the value of the fractional order parameter α, the faster the system reaches the equilibrium point. Although the value of α affects the speed of convergence, it does not affect the stability of the equilibrium point.

Keywords: *Antibiotics, Caputo-Fabrizio, Fractional, Mycobacterium tuberculosis, Numerical simulation*

: https://doi.org/10.30598/parameterv4i1pp233-248

1. INTRODUCTION

Tuberculosis (TB) is one of the most dangerous infectious diseases, with a high global mortality rate [1][2]. Mycobacterium tuberculosis (Mtb) is transmitted through the air when individuals with TB sneeze, cough, or spit in public, allowing others to inhale the bacteria and become infected [3][4]. Approximately 1.6 million people died from tuberculosis (TB) in 2021, including 187,000 individuals who were HIV-positive. The World Health Organization (WHO) reported that there were 10.6 million TB cases worldwide, affecting 1.2 million children, 3.4 million women, and 6 million men [5]. Indonesia ranks third in the world for TB cases, after India and China. The Global TB Report 2021 recorded 824,000 TB cases in Indonesia, but only 393,323 were detected and treated. In 2022, treatment coverage reached 39%, with a treatment success rate of 74% [6]. The Government of Indonesia aims to reduce the incidence of TB, which in 2017 stood at 393,444 per 100,000 population to 190 per 100,000 population by 2024, primarily through improving access to and quality of health services [7].

Mycobacterium tuberculosis (Mtb) is a facultative intracellular pathogen that grows slowly and is capable of surviving within macrophages and other mammalian cells. Infection typically begins in the lungs but may disseminate through the bloodstream or lymphatic system to other organs. Upon entry into the body, macrophages attempt to eliminate the bacteria with assistance from T cells and other components of the immune system [8] [9]. Mtb can be classified as either antibiotic-sensitive or antibiotic-resistant. Infected macrophages are eventually destroyed by T cells, although these cells are not able to directly kill the bacteria. The immune response, particularly the activity of white blood cells, plays a critical role in controlling *Mtb* infection; an increased white blood cell count enhances macrophage effectiveness [10]. T cells, especially $CD4^+$ and $CD8^+$ subsets, are central to this immune defense: $CD4^+$ T cells help activate various immune components, while $CD8^+$ T cells directly target and destroy infected host cells [11].

An increase in infected macrophages, particularly those harboring drug-resistant bacteria, can result from bacterial infection. Mycobacterium tuberculosis develops resistance through spontaneous genetic mutations, which vary depending on the type of antibiotic used [12]. Patients with untreated active TB may carry drug-resistant strains of the disease. For instance, isoniazid resistance may require prolonged therapy, although various combinations of anti-TB drugs can still lead to successful treatment outcomes [13].

Mathematical modeling has been extensively applied across various disciplines, including biology, economics, and health sciences, as a powerful tool for representing real-world phenomena through systems of equations. In the context of infectious diseases, modeling facilitates a deeper understanding of transmission dynamics and enables the evaluation of intervention strategies [14][15]. The behavior of Mycobacterium tuberculosis (Mtb), particularly antibiotic-sensitive strains, has been the focus of numerous studies. For instance, [13] explored the interaction between sensitive and resistant bacteria and their impact on the immune response. Additionally, [16] analyzed the stability and existence of periodic solutions in a bacterial resistance model driven by mutation and plasmid transfer. In another study, [17] investigated the growth dynamics of both intracellular and extracellular Mtb bacteria.

The use of Fractional Differential Equation Systems (FDES), a generalization of Ordinary Differential Equation Systems (ODES), has emerged as an alternative approach in infectious disease modeling. This shift is motivated by the complexity of many biological systems, which are inherently nonlinear and often not solvable through analytical methods. FDES provides a more realistic framework for simulating disease dynamics by incorporating memory effects that are characteristic of biological processes. Furthermore, by reducing errors associated with

neglected parameters, stability analysis within the FDES framework enables more accurate predictions compared to traditional ODES models [18].

Building on previous research, this study aims to integrate the models presented in [13] and [14] into a novel mathematical framework that captures the interaction dynamics and treatment effects of antibiotics on Mycobacterium tuberculosis using a Fractional Differential Equation System (FDES). The analysis focuses on identifying and examining the equilibrium points of the system, supported by numerical simulations, with the goal of providing deeper insights into infection dynamics and the impact of antibiotic interventions.

2. METHODS

This study employed a mathematical modeling approach based on a Fractional Differential Equation System (FDES) to analyze the dynamics between Mycobacterium tuberculosis (Mtb), macrophages, and antibiotic treatment. The model included four key variables: healthy or uninfected macrophages ($\boldsymbol{M_U}$), infected macrophages ($\boldsymbol{M_I}$), antibiotic-sensitive Mtb bacteria ($\boldsymbol{B_S}$), and antibiotic-resistant Mtb bacteria ($\boldsymbol{B_R}$). These interactions were represented by a system of nonlinear fractional differential equations that incorporate both Caputo and Caputo–Fabrizio operators to capture memory effects inherent in biological processes [19].

Mtb infects about one-third of the global population, although only 10% develop active TB. Inadequate treatment can lead to multidrug-resistant TB (MDR-TB), especially if treatment is discontinued or administered inappropriately. Modelling such resistance was important for evaluating control strategies. This study followed the following steps:

1) Flow Diagram: A visual representation of the compartmental transitions is provided to clarify the structure of the system dynamics.
2) Model Formulation: The system of equations is constructed based on the biological interactions between macrophages and *Mycobacterium tuberculosis* (Mtb), including both sensitive and resistant strains.
3) Definition of Fractional Operators: The Caputo and Caputo–Fabrizio derivatives are employed to incorporate long-term memory effects in the model.
4) Equilibrium Analysis: Disease-free and endemic equilibrium points are determined by setting the rate of change in the system to zero.
5) Basic Reproduction Number (R_0): Computed using the next-generation matrix approach as an indicator of the infection's transmission potential
6) System Stability: Local stability is analyzed through system linearization using the Jacobian matrix and evaluating its eigenvalues.
7) Stability Analysis Based on R_0: The infection dynamics are assessed based on the value of R_0, whether the infection dies out ($R_0 < 1$) or persists ($R_0 > 1$), determined through the eigenvalues of the Jacobian matrix.
8) Numerical Simulation: Implemented using the three-step Adams–Bashforth method for the Caputo–Fabrizio operator to visually and numerically verify the analytical results.

3. RESULTS AND DISCUSSIONS

3.1. Model Formulation

This study presented a mathematical model that describes the interaction dynamics and the effects of antibiotic treatment on Mycobacterium tuberculosis. The model included four variables: healthy or uninfected macrophages (M_U), infected macrophages (M_I), antibiotic-sensitive Mycobacterium tuberculosis (B_S), and antibiotic-resistant Mycobacterium tuberculosis (B_R). These components are illustrated in the schematic diagram shown in **Figure 1** below:

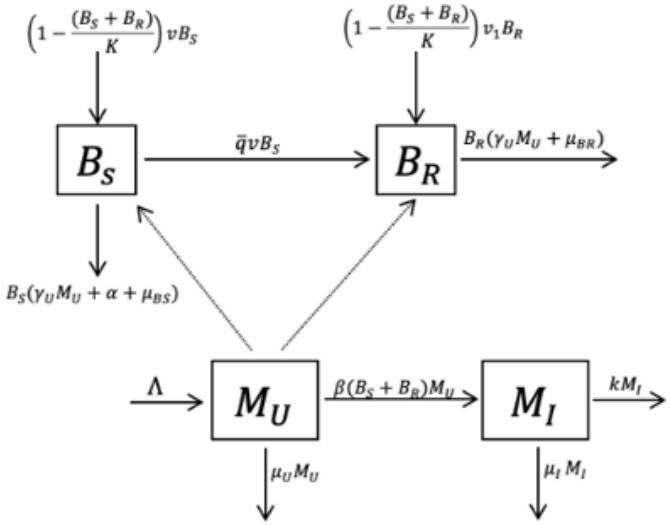

Figure 1. Schematic diagram of macrophage and bacteria interaction.

In **Figure 1**, the population of uninfected macrophages, $M_U(t)$, was influenced by several factors: the recruitment rate of uninfected macrophages per unit of time, denoted by Λ; the natural death rate, represented by $\mu_U M_U(t)$; and the rate of interaction between uninfected macrophages and both sensitive and resistant bacteria, expressed as $\beta(B_s(t)+B_r(t))M_U(t)$. Accordingly, the mathematical equation describing the dynamics of uninfected macrophages was given as follows:

$$\frac{dM_U(t)}{dt} = \Lambda - \beta(B_s(t)+B_r(t))M_U(t) - \mu_U M_U(t) \quad (1)$$

The population of infected macrophages, $M_I(t)$, was influenced by several factors: the interaction between uninfected macrophages and both sensitive and resistant bacteria per unit of time, represented by $\beta(B_s(t)+B_r(t))M_U(t)$; the natural death rate of infected macrophages per unit of time, given by $\mu_I M_I(t)$; and the death of infected macrophages due to T cell activity per unit of time, expressed as $kM_I(t)$. The corresponding mathematical equation for infected macrophages was given as follows:

$$\frac{dM_I(t)}{dt} = \beta(B_s(t)+B_r(t))M_U(t) - \mu_I M_I(t) - kM_I(t) \quad (2)$$

The population of Mycobacterium tuberculosis bacteria that are sensitive to antibiotics, denoted by $B_S(t)$ was influenced by several factors per unit of time. First, the sensitive bacteria grow at a rate v with a maximum carrying capacity K, represented by the logistic growth term $\left(1-\frac{(B_S(t)+B_R(t))}{K}\right)vB_S(t)$. Second, the population of sensitive bacteria decreases due to mutation, where a fraction of replicating bacteria becomes antibiotic-resistant, represented by $qvB_S(t)$.

Third, the population is also reduced due to natural death, phagocytosis or destruction by uninfected macrophages, and antibiotic administration, represented by $(\gamma_U M_U + \alpha + \mu_{BS})B_S(t)$. The resulting equation for the antibiotic-sensitive bacterial population was expressed as follows:

$$\frac{dB_S(t)}{dt} = \left(1 - \frac{(B_S(t)+B_R(t))}{K}\right) vB_S(t) - qvB_S(t) - (\gamma_U M_U + \alpha + \mu_{BS})B_S(t) \quad (3)$$

The population of antibiotic-resistant bacteria, denoted by $B_R(t)$, was influenced by several factors per unit of time. First, resistant bacteria grow at a rate v_1 with a maximum carrying capacity K, represented by the logistic growth term $\left(1 - \frac{(B_S(t)+B_R(t))}{K}\right) v_1 B_R(t)$. Second, the population of resistant bacteria increases due to the mutation of sensitive bacteria into resistant strains, represented by $qvB_S(t)$. Third, the resistant bacterial population decreases due to natural death and elimination by uninfected macrophages, expressed as $(\gamma_U M_U + \mu_{BR})B_R(t)$. The resulting equation for the antibiotic-resistant bacterial population was formulated as follows:

$$\frac{dB_R(t)}{dt} = \left(1 - \frac{(B_S(t)+B_R(t))}{K}\right) v_1 B_R(t) + qvB_S(t) - (\gamma_U M_U + \mu_{BR})B_R(t) \quad (4)$$

3.2. Non-Dimensionalisation

To reduce the number of parameters, the system was simplified by applying non-dimensionalisation through following variable transformations:

$$M_U = \frac{M_U}{\Lambda/\mu_U} \; ; \; M_I = \frac{M_I}{\Lambda/\mu_U} \; ; \; B_S = \frac{B_S}{K} \; ; \; B_R = \frac{B_R}{K}.$$

In accordance with **Equations (1)-(4)**, new variables were introduced through substitution, resulting in the following system of differential equations:

$$\begin{aligned}
\frac{dM_U(t)}{dt} &= \mu_U - \beta(B_s(t) + B_r(t))M_U(t) - \mu_U M_U(t) \\
\frac{dM_I(t)}{dt} &= \beta(B_s(t) + B_r(t))M_U(t) - \mu_I M_I(t) - kM_I(t) \\
\frac{dB_S(t)}{dt} &= \big(1 - (B_S(t) + B_R(t))\big)vB_S(t) - qvB_S(t) \\
&\quad - (\gamma_U M_U + \alpha + \mu_{BS})B_S(t) \\
\frac{dB_R(t)}{dt} &= \big(1 - (B_S(t) + B_R(t))\big)v_1 B_R(t) + qvB_S(t) - (\gamma_U M_U + \mu_{BR})B_R(t)
\end{aligned} \quad (5)$$

3.3. Fractional Model

To incorporate the memory effect inherent in the dynamic system, the interaction and antibiotic response model of Mycobacterium tuberculosis, as described in **Equation (5)**, was generalized by replacing the integer-order derivative with a non-integer (fractional) derivative. Specifically, the first-order time derivative $\frac{d}{dt}$ was replaced with the Caputo–Fabrizio fractional derivative D_t^{α}, where $\alpha \in (0,1)$ denotes the order of the derivative. As a result, the fractional differential equation model describing the interaction dynamics of Mycobacterium tuberculosis and antibiotics for $t > 0$ was formulated as follows:

$${}^{CF}D_t^{\alpha} M_U(t) = \mu_U - \beta(B_s(t) + B_r(t))M_U(t) - \mu_U M_U(t)$$

$$
\begin{aligned}
{}^{CF}D_t^{\alpha} M_I(t) &= \beta(B_s(t) + B_r(t))M_U(t) - \mu_I M_I(t) - kM_I(t) \\
{}^{CF}D_t^{\alpha} B_S(t) &= \Big(1 - \big(B_S(t) + B_R(t)\big)\Big) vB_S(t) - qvB_S(t) - (\gamma_U M_U + \alpha + \mu_{BS})B_S(t) \\
{}^{CF}D_t^{\alpha}(t) &= \big(1 - (B_S(t) + B_R(t))\big)v_1 B_R(t) + qvB_S(t) - (\gamma_U M_U + \mu_{BR})B_R(t),
\end{aligned} \tag{6}
$$

with the initial condition $M_U(0) \geq 0, M_I(0) \geq 0, B_S(0) \geq 0, B_R(0) \geq 0$.

3.4. Equilibrium points

By algebraic manipulation, the equilibrium point was obtained, resulting in the Infection-Free Equilibrium Point $\boldsymbol{E_0}$ as follows:

$$\boldsymbol{E_0} = \big(\boldsymbol{M_U}, \boldsymbol{M_I}, \boldsymbol{B_S}, \boldsymbol{B_R}\big) = (\mathbf{1}, \mathbf{0}, \mathbf{0}, \mathbf{0})$$

Next, to determine the basic reproduction number (R_0), the next-generation matrix method was used. This yielded the following expression for R_0:

$$R_0 = \max\{R_1, R_2\}$$

where,

$$R_1 = \frac{v}{qv + \gamma_U + \alpha + \mu_{BS}}, R_2 = \frac{v_1}{\gamma_U + \mu_{BR}}.$$

Furthermore, the endemic equilibrium point can be analyzed based on the equations derived from the infection-free equilibrium point E_0. The endemic equilibrium consisted of two types: the infection equilibrium point E_1 and the coexistence infection equilibrium point E_2. **Table 1** presented a summary of the derived endemic equilibrium points:

Table 1. Endemic equilibrium points

Symbol	Type	Equilibrium point
E_1	Infected equilibrium point	$({M_U}^*, {M_I}^*, 0, {B_R}^*)$
E_2	Coexistence infected equilibrium point	$({M_U}^{**}, {M_I}^{**}, {B_S}^{**}, {B_R}^{**})$

where,

$${M_U}^* = \frac{\mu_U}{(\beta {B_R}^* + \mu_U)}, {M_I}^* = \frac{\beta {B_R}^* \mu_U}{(\beta {B_R}^* + \mu_U)(\mu_I + k)}, {M_U}^{**} = \frac{\mu_U}{\beta({B_S}^{**} + {B_R}^{**}) + \mu_U},$$

$${M_I}^{**} = \frac{\beta({B_S}^{**} + {B_R}^{**})\mu_U}{(\beta({B_S}^{**} + {B_R}^{**}) + \mu_U)(\mu_I + k)},$$

and ${B_R}^*$ are the positive real roots of the equation $a_2 {B_R}^2 + a_1 B_R + a_0 = 0$, ${B_S}^{**}$ are the positive real roots of the equation $b_2 {B_S}^2 + b_1 B_S + b_0 = 0$, and ${B_R}^{**}$ are the positive real roots of the equation $c_3 {B_R}^3 + c_2 {B_R}^2 + c_1 B_R + c_0 = 0$.

3.5. Analysis of equilibrium point stability

3.5.1. Stability of the equilibrium point $\boldsymbol{E_0}$

The stability analysis of the equilibrium point E_0 is given in **Theorem 1.**

Theorem 1. *The infection-free equilibrium point E_0 is locally asymptotically stable if $R_0 < 1$.*

Proof. By linearizing **Equation (6)** and calculating the Jacobian matrix of the system at point $E_0 = (M_U, M_I, B_S, B_R) = (1,0,0,0)$, we obtain

$$J(E_0) = \begin{pmatrix} -\mu_U & 0 & -\beta & -\beta \\ 0 & -\mu_I - k & \beta & \beta \\ 0 & 0 & v - qv - \gamma_U - \alpha - \mu_{BS} & 0 \\ 0 & 0 & qv & v_1 - \gamma_U - \mu_{BR} \end{pmatrix}$$

with eigen values:

$\lambda_1 = -\mu_U$

$\lambda_2 = -\mu_I - k$

$\lambda_3 = v - qv - \gamma_U - \alpha - \mu_{BS} = (R_1 - 1)(qv + \gamma_U + \alpha + \mu_{BS})$

$\lambda_4 = v_1 - \gamma_U - \mu_{BR} = (R_2 - 1)(\gamma_U + \mu_{BR})$

where $R_1 = \frac{v}{qv+\gamma_U+\alpha+\mu_{BS}}, R_2 = \frac{v_1}{\gamma_U+\mu_{BR}}$, so $R_0 = \max\{R_1, R_2\}$. If $R_0 < 1$ then $R_1 < 1$ and $R_2 < 1$, so that all of the eigenvalues are negative. Then, E_0 locally asymptotically stable if $R_0 < 1$.

3.5.2. Stability of the equilibrium point E_1

The stability analysis of the equilibrium point E_1 is given in **Theorem 2.**

Theorem 2. *The equilibrium point* $E_1 = ({M_U}^*, {M_I}^*, 0, {B_R}^*)$ *locally asymptotically stable if* $R_2 > 1$ *and* $v(1 - {B_R}^*) < qv + \gamma_U {M_U}^* + \alpha + \mu_{BS}$, $s_2 s_1 - s_0 > 0$.

Proof. The Jacobian matrix at the equilibrium point E_1 is:

$$J(E_1) = \begin{pmatrix} -F & 0 & -P & P \\ G & -L & P & -P \\ 0 & 0 & Q - R & 0 \\ -I & 0 & -T & W - X \end{pmatrix}$$

with

$F = \beta {B_R}^* + \mu_U$; $G = \beta {B_R}^*$; $I = \gamma_U {B_R}^*$; $L = \mu_I + k$; $P = \beta {M_U}^*$;

$Q = v(1 - {B_R}^*)$; $R = qv + \gamma_U {M_U}^* + \alpha + \mu_{BS}$; $T = v_1 {B_R}^* + qv$;

$W = v_1(1 - 2{B_R}^*)$; $X = \gamma_U {M_U}^* + \mu_{BR}$;

The characteristic equation is

$(\lambda - Q + R)(\lambda^3 + \lambda^2 s_2 + \lambda s_1 + s_0) = 0$

where:

$s_2 = X + F + L - W$

$s_1 = FX + LX + FL - FW - LW$

$s_0 = FL(X - W)$

The first eigenvalue is:

$$\lambda_1 = Q - R = v(1 - {B_R}^*) - (qv + \gamma_U {M_U}^* + \alpha + \mu_{BS})$$

and the other three eigenvalues are the roots of a cubic equation:

$$\lambda^3 + s_2 \lambda^2 + s_1 \lambda + s_0 = 0$$

So we find that $\lambda_1 < 0$ if $v(1-{B_R}^*) < (qv+\gamma_U {M_U}^* + \alpha\,\mu_{BS})$ and according to the Routh-Hurwitz criterion, all of the eigenvalues will have a negative real part if $s_2, s_{1,} s_0 > 0$, $s_2 s_1 - s_0 > 0$. This condition will be fulfilled if $|\arg(\lambda_i)| > \frac{\alpha\pi}{2}, i = 1,2,3$. Thus, the equilibrium point E_1 will be locally asymptotically stable $R_2 > 1$ and $v(1-{B_R}^*) < qv+\gamma_U {M_U}^* + \alpha + \mu_{BS}$, $s_2 s_1 - s_0 > 0$.

3.5.3 Stability of the equilibrium point E_2

The stability analysis of the equilibrium point E_2 is given in **Theorem 3**.

Theorem 3. *The equilibrium point* $E_2 = ({M_U}^{**}, {M_I}^{**}, {B_S}^{**}, {B_R}^{**})$ *locally asymptotically stable if* $R_1 > 1, R_2 > 1,\ y_3 > 0,\ y_3 y_2 - y_1 > 0,$ *and* $y_3 y_2 y_1 - {y_3}^2 y_0 - {y_1}^2 > 0$.

Proof. The Jacobian matrix at the equilibrium point E_2 is:

$$J(E_2) = \begin{pmatrix} -F-\mu_U & 0 & -J & -J \\ F & -I & J & J \\ -G & 0 & Q-R & -Z \\ -H & 0 & -T+qv & W-X \end{pmatrix},$$

with

$F = \beta {B_S}^{**} + \beta {B_R}^{**}$; $G = \gamma_U {B_S}^{**}$; $H = \gamma_U {B_R}^{**}$; $I = \mu_I + k$; $J = \beta {M_U}^*$;

$Q = v(1-2{B_S}^{**} - {B_R}^{**})$; $R = qv + \gamma_U {M_U}^{**} + \alpha + \mu_{BS}$; $T = v_1 {B_R}^{**}$;

$W = v_1(1-2{B_R}^{**} - {B_S}^{**})$; $X = \gamma_U {M_U}^{**} + \mu_{BR}$; $Z = vB_S$.

The characteristic equation is:

$$\lambda^4 + y_3\lambda^3 + y_2\lambda^2 + y_1\lambda + y_0 = 0,$$

with

$y_3 = F + \mu_U + R + X + 1 - Q - W$

$y_2 = (F+\mu_U)(R+X+1-Q-W) + WQ + RX + R - JG - WR - XQ - Q - W - X$

$y_1 = \mu_U(WQ + XR + R - RW - XQ - Q - W - X) + F(WQ + XR - XQ - Q - W - R - X) + JGW + JG + QW + QX - XJG - RW - RX$

$y_0 = \mu_U(QW + QX - RW - RX) + F(QW + QX - RX) + JG(W + X)$

According to the Routh-Hurwitz criterion, all of the eigenvalues have a negative real part if and only if $y_3 > 0,\ y_3 y_2 - y_1 > 0$ and $y_3 y_2 y_1 - {y_3}^2 y_0 - {y_1}^2 > 0$, which fulfilled if $|\arg(\lambda_i)| > \frac{\alpha\pi}{2}, i = 1,2,3,4, R_1 > 1, R_2 > 1$.

3.6. Numerical results

3.6.1. Simulation with the System of Differential Equations of order 1

In this section, a numerical simulation was conducted to examine the stability of the infection-free equilibrium point E_0, using a system of ordinary differential equations (first-order). The simulation employed the parameter value $v_1 = 0.1$, with a time interval from $t = 0$ to $t = 400$, and a step size of 0.2. The initial conditions were set as follows: $M_U(0) = 0.3$, $M_I(0) = 0.2, B_S(0) = 0.1, B_R(0) = 0.7$. The purpose of the simulation was to observe the interactions

among these components over time and determined whether the system converges to the infection-free equilibrium. The graph in **Figure 2** illustrated the dynamics of M_U , M_I , B_S, and B_R with respect to time t. In other words, **Figure 2** illustrated the interaction between uninfected macrophages, infected macrophages, antibiotic-sensitive Mycobacterium tuberculosis (Mtb), and antibiotic-resistant Mtb bacteria. The populations of infected macrophages, sensitive bacteria, and resistant bacteria declined toward zero because of the antibiotic's effectiveness in reducing the bacterial load. Meanwhile, the population of uninfected macrophages increased and approached one.

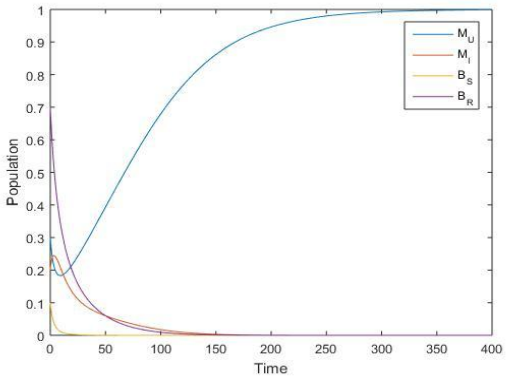

Figure 2. Interaction graph of M_U, M_I, B_S, and B_R over time t under the condition $R_0 < 1$.

Figures 3 and **Figure 4** presented the stability of the infection-free equilibrium point E_0 under various initial conditions. **Figure 3** showed simulations using different initial values, where the trajectories of uninfected macrophages and both sensitive and resistant bacterial populations converge toward the equilibrium point E_0. **Figure 4** illustrated the population dynamics under another set of initial conditions, revealing that infected macrophages, sensitive bacteria, and resistant bacteria all move toward the infection-free equilibrium point $E_0 = (1,0,0,0)$ with $R_0 = 0.5$. This indicated that, on average, each newly infected macrophage leads to less than one secondary infection per day. Therefore, the equilibrium point E_0 is locally asymptotically stable for $R_0 < 1$, in accordance with **Theorem 1**.

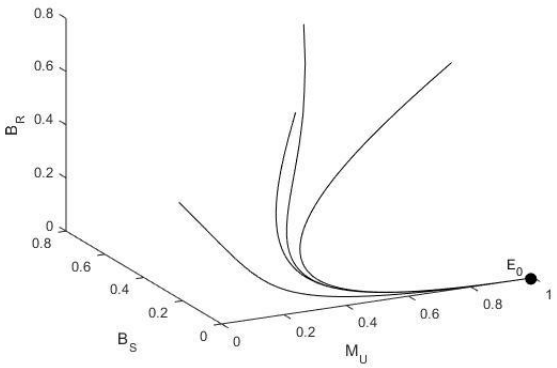

Figure 3. The graphs of M_U, B_S, B_R with different initial values converge to the point E_0 when $R_0 < 1$

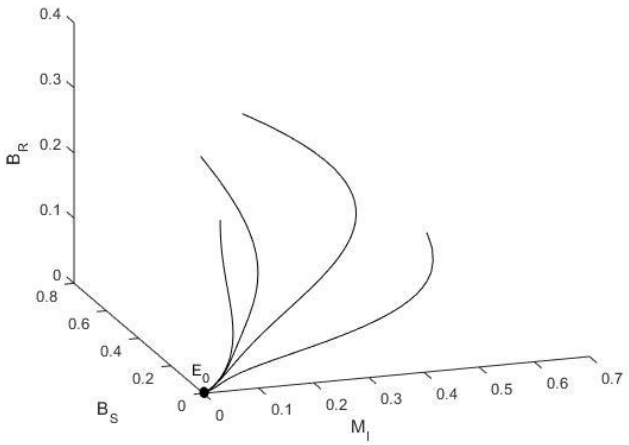

Figure 4. The graphs of M_I, B_S, B_R with different initial values converge to the point E_0 when $R_0 < 1$.

Next, a numerical simulation was carried out to examine the stability of the equilibrium point $E_1 = (M_U{}^*, M_I{}^*, 0, B_R{}^*)$, using the parameter value $v_1 = 0.25$. The model based on a first-order system of ordinary differential equations. The simulation was run over the time interval $t = 0$ to $t = 400$ with a step size of 0.2. The initial conditions were set as follows: $M_U(0) = 0.3\,, M_I(0) = 0.2, B_S(0) = 0.1, B_R(0) = 0.7$. **Figure 5** illustrated the interaction of $M_U\,, M_I\,, B_S$, and B_R over time t. It can be observed that the population of antibiotic-resistant bacteria increased over time, leading to a corresponding rise in the number of infected macrophages. Meanwhile, the population of uninfected macrophages declined due to the active presence of resistant bacteria, which continue to infect healthy macrophages. In contrast, the population of antibiotic-sensitive bacteria decreased and approached zero. This decline was caused by the effect of antibiotics, which effectively kill or suppress sensitive bacteria. While antibiotics successfully reduced the population of sensitive bacteria, they had no effect on resistant strains, allowed the resistant bacteria to persist and become dominant.

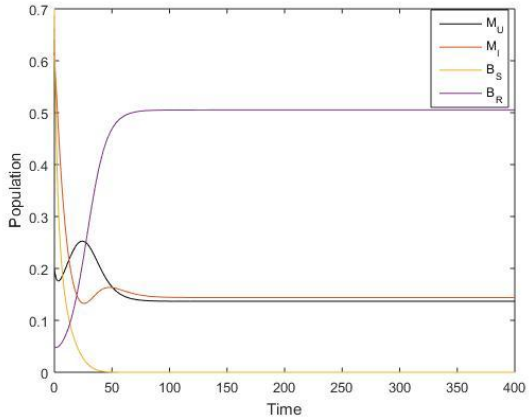

Figure 5. Interaction graph of M_U, M_I, B_S, and B_R over time t under the condition $R_2 > 1$

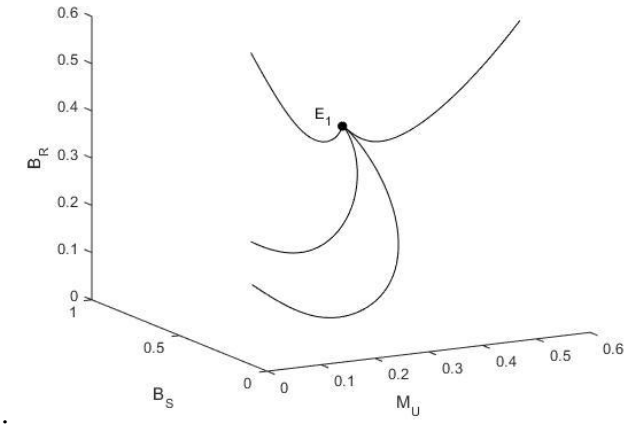

Figure 6. The graphs of M_U, B_S, B_R with different initial values converge to the point E_1.

The stability of the equilibrium point E_1 under various initial conditions was illustrated in the next two figures. **Figure 6** demonstrated that uninfected macrophages, sensitive bacteria, and antibiotic-resistant bacteria evolved toward the equilibrium point E_1. **Figure 7** further confirmed that infected macrophages, sensitive bacteria, and resistant bacteria converged to the equilibrium point $E_1 = (0.136697\,, 0.143885\,, 0\,,\ 0.505237)$, with a basic reproduction number $R_2 = 1.7$. This indicated that the populations of uninfected macrophages, infected macrophages, sensitive bacteria, and resistant bacteria stabilized at this endemic equilibrium. The value $R_2 = 1.7$, suggested that, on average, each newly infected macrophage gives rise to at least 1.7 additional infections per day. These results confirmed that the equilibrium point E_1 is locally asymptotically stable.

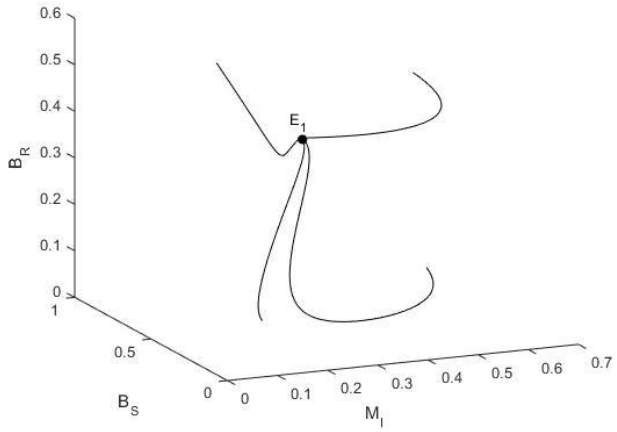

Figure 7. The graphs of M_I, B_S, B_R with different initial values converge to the point E_1.

Next, to demonstrate the stability of the equilibrium point $E_2 = (M_U{}^{**}, M_I{}^{**}, B_S{}^{**}, B_R{}^{**})$, simulations were carried out using the parameter values $v = 0.9$ and $v_1 = 0.3$. This simulation used a first-order system of ordinary differential equations. The time interval considered from $t = 0$ to $t = 400$, with a step size of 0.2. The initial conditions were set as follows: $M_U(0) =$

$0.3\,, M_I(0) = 0.2, B_S(0) = 0.1, B_R(0) = 0.7$. The interaction dynamics of $M_U\,, M_I\,, B_S,$ and B_R over time t are illustrated in **Figure 8**.

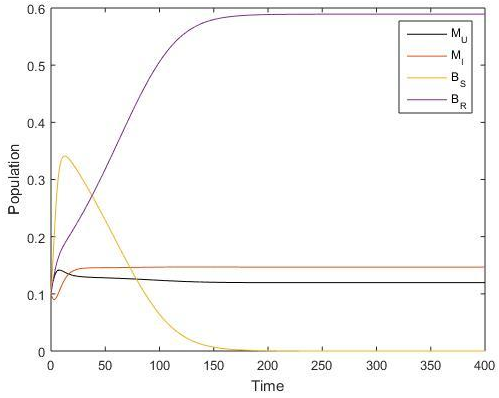

Figure 8. Interaction graph of M_U, M_I, B_S, and B_R over time t under the condition $R_1 > 1$ and $R_2 > 1$

In **Figure 8**, it can be observed that the population of antibiotic-resistant bacteria continued to increase, leading to a rise in the number of infected macrophages over time. Meanwhile, the population of antibiotic-sensitive bacteria began to decline and approached zero around day 300, because of antibiotics that eliminate sensitive bacteria. The population of uninfected macrophages also decreased, as active resistant bacteria continued to infect them.

The stability of the equilibrium point E_2 under various initial conditions was also illustrated in in the next two figures. **Figure 9** showed that uninfected macrophages, sensitive bacteria, and resistant bacteria moved toward the equilibrium point E_2. **Figure 10** further demonstrated that infected macrophages, sensitive bacteria, and resistant bacteria also converged to the equilibrium point $E_2 = (0.118965\,, 0.146875\,, 0.0029726\,,\ 0.584981)$, with basic reproduction numbers $R_1 = 2$ and $R_2 = 2$. This implied that, on average, each newly infected macrophage led to at least two new infections per day. The results confirmed that all state variables, uninfected macrophages, infected macrophages, sensitive bacteria, and resistant bacteria, stabilized at the endemic equilibrium point, E_2, indicated that E_2 is locally asymptotically stable.

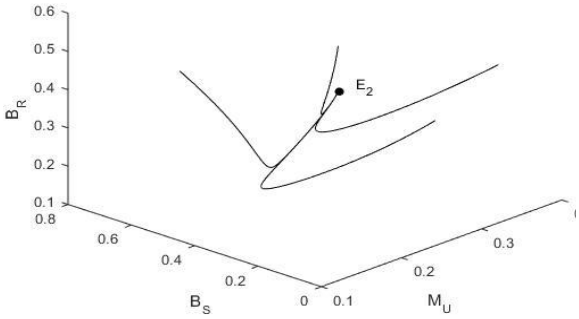

Figure 9. The graphs of M_U, B_S, B_R with different initial values converge to the point E_2

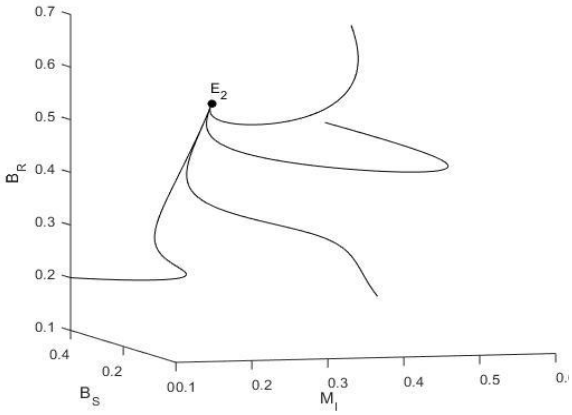

Figure 10. The graphs of M_I, B_S, B_R with different initial values converge to the point E_2

The equilibrium points E_1 and E_2 suggested that the number of infected macrophages could exceed that of uninfected macrophages. The existence of these endemic equilibria was possible only if the population of resistant bacteria could survive immune responses, allowed them to remain active within the host. Both the infection-free equilibrium and the locally stable endemic equilibria were asymptotically stable, indicated that the system tends to settle into a steady state without reactivating latent infection or disrupting the bacterial clearance process. While antibiotics contributed to the reduction or elimination of antibiotic-sensitive bacteria, they had limited effect on resistant strains. As a result, resistant bacteria persisted in the system, highlighted the need for additional or alternative treatment strategies beyond antibiotic therapy alone.

3.6.2. Simulation with a fractional differential equation system

In this simulation, several fractional orders are used, $\alpha = 0.6, 0.7, 0.9$, and 1, with the initial conditions $M_U(0) = 0.3\,, M_I(0) = 0.2, B_S(0) = 0.1$, and $B_R(0) = 0.7$, along with a fixed set of parameter values. The simulation results, illustrated in **Figure 11**, showed that the uninfected macrophage population converges toward the equilibrium point for all values of α. Notably, for the same initial conditions, the system with $\alpha = 0.6$ reached the equilibrium faster than those with $\alpha = 0.7, 0{,}9,$ and 1. This highlighted the significant influence of the fractional order on the convergence rate of the system.

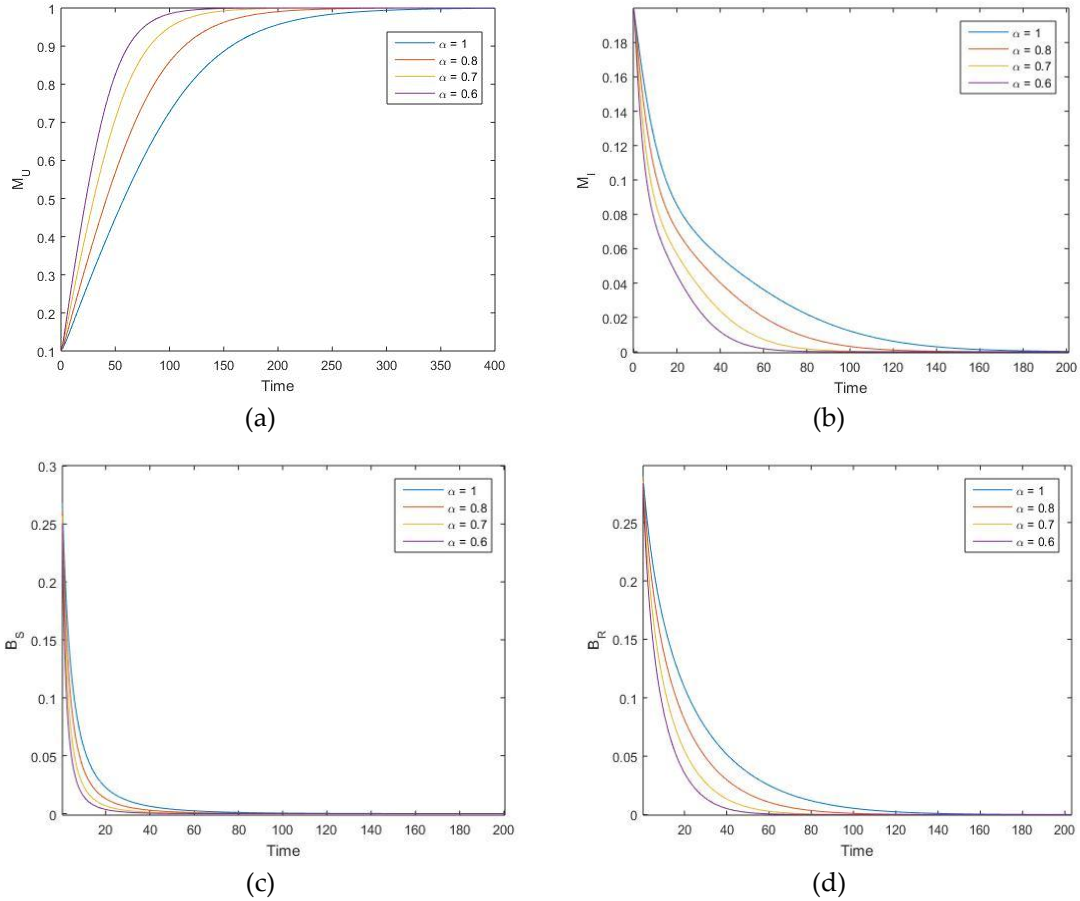

Figure 11. Population dynamics with different orders: (a) uninfected macrophages (M_U), (b) infected macrophages (M_I), (c) antibiotic-sensitive Mtb bacteria (B_S), and (d) antibiotic-resistant Mtb bacteria (B_R).

As shown in **Figure 11**, the populations of uninfected macrophages, infected macrophages, antibiotic-sensitive bacteria, and antibiotic-resistant bacteria all converged toward their respective equilibrium points under varying fractional orders. With identical initial conditions, the system with $\alpha = 0.6$ consistently reached equilibrium faster than those with $\alpha = 0.7, 0.8$, and 1. This result suggested that lower fractional orders accelerated the system's convergence to equilibrium. The underlying reason lied in the memory effect intrinsic to the Caputo-Fabrizio fractional derivative: smaller values of α placed greater weight on historical system behavior, thereby enhanced the damp of fluctuations and speed up stabilization.

This finding aligned with the results reported in **[20]**, which demonstrated that a fractional-order model with $\alpha = 0.93$ provided a better fit to empirical data compared to a classical integer-order model, and improved predictive accuracy by 28.5%. Additionally, research by **[21]** confirmed that the use of Caputo-Fabrizio derivatives in tuberculosis modeling yielded stable solutions and faster convergence relative to traditional approaches. These insights highlighted the potential utility of fractional-order models in the design of more effective and stable tuberculosis treatment strategies.

4. CONCLUSION

This paper presents a fractional-order mathematical model based on Caputo-Fabrizio derivatives to describe the dynamics of the interaction between Mycobacterium tuberculosis (Mtb) and antibiotic treatment, explicitly distinguishing between antibiotic-sensitive and antibiotic-resistant bacterial strains. Compared to conventional integer-order models, the fractional-order approach offers a more accurate depiction of biological processes by incorporating memory effects that are intrinsic to biological systems. The model introduces a basic reproduction number R_0 as a threshold for disease control and identifies three equilibrium points: a disease-free equilibrium and two endemic equilibria. Stability analysis of these equilibriums is conducted through linearization and eigenvalue examination. Numerical simulations are performed using the three-step Adams-Bashforth method adapted for Caputo-Fabrizio derivatives. The results indicate that the system converges to an equilibrium point regardless of variations in initial conditions. Notably, the fractional order parameter α plays a significant role in the convergence behavior; smaller values of α lead to faster convergence. This finding underscores the importance of memory effects in disease dynamics, which are overlooked in classical models. Overall, the fractional-order model enhances both analytical precision and biological realism, offering new insights for the development of more effective antibiotic treatment strategies, particularly in addressing antibiotic resistance. Future research should consider incorporating immune system interactions, combination drug therapies, and spatial heterogeneity to broaden the applicability of the model to more complex clinical and epidemiological contexts.

ACKNOWLEDGMENTS

The authors would like to thank Joko Purwadi, UAD, for proofreading the manuscript and providing valuable feedback. Consent has been obtained from the individual acknowledged.

FUNDING INFORMATION

The authors state that no external funding is involved. The authors themselves provided full support and funding for all of the study's associated activities.

CONFLICT OF INTEREST STATEMENT

The authors state no conflict of interest.

INFORMED CONSENT

This study does not involve any individual participant data, and no informed consent was required.

ETHICAL APPROVAL

There were no ethical issues with this research because it didn't involve experimentation on people or animals.

DATA AVAILABILITY

This study is based on hypothetical data used for simulation purposes only. No real-world data were used or analyzed.

REFERENCES

[1] K. Alanazi *et al.*, "Navigating tuberculosis control: A mathematical approach to disease dynamics and vaccination strategies," *Alexandria Eng. J.*, vol. 121, no. November 2024, pp. 183–192, 2025, doi: 10.1016/j.aej.2025.02.053.

[2] B. Jima, D. Hailu, and G. Dejene, "The magnitude of health care seeking delay and associated factors for tuberculosis suggestive symptoms in Sidama Region Ethiopia: Community-based cross-sectional study," *Public Heal. Pract.*, vol. 6, no. May, p. 100441, 2023, doi: 10.1016/j.puhip.2023.100441.

[3] A. A. J. Aljanaby, Q. M. H. Al-Faham, I. A. J. Aljanaby, and T. H. Hasan, "Epidemiological study of Mycobacterium Tuberculosis in Baghdad Governorate, Iraq," *Gene Reports*, vol. 26, 2022, doi: 10.1016/j.genrep.2021.101467.

[4] K. M. Owolabi and E. Pindza, "A nonlinear epidemic model for tuberculosis with Caputo operator and fixed point theory," *Healthc. Anal.*, vol. 2, no. September, p. 100111, 2022, doi: 10.1016/j.health.2022.100111.

[5] World Health Organization, "mycobacterium tuberculosis," *WHO*, 2022. .

[6] Kementrian Kesehatan RI, "Tuberkulosis," 2022. .

[7] Kementrian Kesehatan RI, "Strategi Nasional Penanggulangan Tuberkulosis di Indonesia.," 2020. .

[8] G. Magombedze, W. Garira, and E. Mwenje, "Modelling the human immune response mechanisms to mycobacterium tuberculosis infection in the lungs," *Math. Biosci. Eng.*, vol. 3, no. 4, pp. 661–682, 2006, doi: 10.3934/mbe.2006.3.661.

[9] R. E. Maphasa, M. Meyer, and A. Dube, "The Macrophage Response to Mycobacterium tuberculosis and Opportunities for Autophagy Inducing Nanomedicines for Tuberculosis Therapy," *Front. Cell. Infect. Microbiol.*, vol. 10, no. February, pp. 1–22, 2021, doi: 10.3389/fcimb.2020.618414.

[10] Kementrian Kesehatan RI, "Fungsi Sel Darah Putih dan Gangguan yang Dapat Terjadi," 2021. .

[11] A. N. Rochmatin and U. Pagalay, "Analisis perilaku dinamik pada sel T CD4+ dan sel T CD8+ terhadap infeksi mikobakterium," *CAUCHY J. Mat. Murni dan Apl.*, vol. 3, no. 2, pp. 72–83, 2014, doi: 10.18860/ca.v3i2.2575.

[12] Y. Zhang and W. W. Yew, "Mechanisms of drug resistance in Mycobacterium tuberculosis," *International Journal of Tuberculosis and Lung Disease*, vol. 13, no. 11. pp. 1320–1330, 2009.

[13] E. Ibargüen-Mondragón and L. Esteva, "On the interactions of sensitive and resistant Mycobacterium tuberculosis to antibiotics," *Math. Biosci.*, vol. 246, no. 1, pp. 84–93, 2013, doi:

10.1016/j.mbs.2013.08.005.
[14] R. S. Imran, R. Resmawan, N. Achmad, and A. R. Nuha, "SEIPR-Mathematical Model of the Pneumonia Spreading in Toddlers with Immunization and Treatment Effects," *J. Mat. Stat. dan Komputasi*, vol. 17, no. 2, pp. 202–218, 2020, doi: 10.20956/jmsk.v17i2.11166.
[15] W. M. Sweileh, "Global research activity on mathematical modeling of transmission and control of 23 selected infectious disease outbreak," *Global. Health*, vol. 18, no. 1, pp. 1–14, 2022, doi: 10.1186/s12992-022-00803-x.
[16] J. L.-E. Justino Alavez-Ramírez, J. Rogelio Avendano Castellanos, Lourdes Esteva, José Antonio Flores, José Luis Fuentes-Allen, Gisela García-Ramos, Guillermo Gómez, "Within-host population dynamics of antibiotic-resistant M. tuberculosis," *A J. IMA*, 2007, doi: 10.1093/imammb/dql026.
[17] E. Ibargüen-Mondragón, L. Esteva, and E. M. Burbano-Rosero, "Mathematical model for the growth of mycobacterium tuberculosis in the granuloma," *Math. Biosci. Eng.*, vol. 15, no. 2, pp. 407–428, 2018, doi: 10.3934/mbe.2018018.
[18] M. I. Utoyo, E. A. Nurafifah, and M. Miswanto, "Analisis Model Matematika Orde Fraksional Penyebaran Worm Berbasis Wi-Fi Pada Smartphone," *Limits J. Math. Its Appl.*, vol. 15, no. 2, p. 97, 2018, doi: 10.12962/limits.v15i2.4304.
[19] I. Petras, *Fractional-Order Nonlinear Systems, Modeling, Analysis and Simulation.* 2011.
[20] S. Bhatter, S. Kumawat, S. D. Purohit, and D. L. Suthar, "Mathematical modeling of tuberculosis using Caputo fractional derivative: a comparative analysis with real data," *Sci. Rep.*, vol. 15, no. 1, pp. 1–19, 2025, doi: 10.1038/s41598-025-97502-5.
[21] S. Ahmad, R. Ullah, and D. Baleanu, "Mathematical analysis of tuberculosis control model using nonsingular kernel type Caputo derivative," *Adv. Differ. Equations*, vol. 2021, no. 1, 2021, doi: 10.1186/s13662-020-03191-x.